High-strength additively manufacturable Al-Zr-Er-Ni alloys with high as-built ductility and thermal stability

Zhaoxuan Ge[1], Shaolou Wei[2], Zehua Liu[1], Tomasz Choma[3,4], Łukasz Żrodowski[3,4], Marc De Graef[1], A. John Hart[5], S. Mohadeseh Taheri-Mousavi[1,6*]

[1]Department of Materials Science and Engineering, Carnegie Mellon University, 5000 Forbes Avenue, Pittsburgh, PA 15213, USA.

[2]Max Planck Institute for Sustainable Materials, Max-Planck-Straße 1, Düsseldorf 40237, Germany

[3]Faculty of Materials Science and Engineering, Warsaw University of Technology, Woloska141 St., 02-507 Warsaw, Poland

[4]Amazemet Sp. z o.o. [Ltd], Al. Jana Pawła II 27, 00-867 Warsaw, Poland

[5]Department of Mechanical Engineering, Massachusetts Institute of Technology, 77 Massachusetts Avenue, Cambridge, MA 02139, USA

[6]Department of Mechanical Engineering, Carnegie Mellon University, 5000 Forbes Avenue, Pittsburgh, PA 15213, USA.

*Corresponding author: S. Mohadeseh Taheri-Mousavi, smtaherimousavi@cmu.edu

Supplementary Information:

Figures:

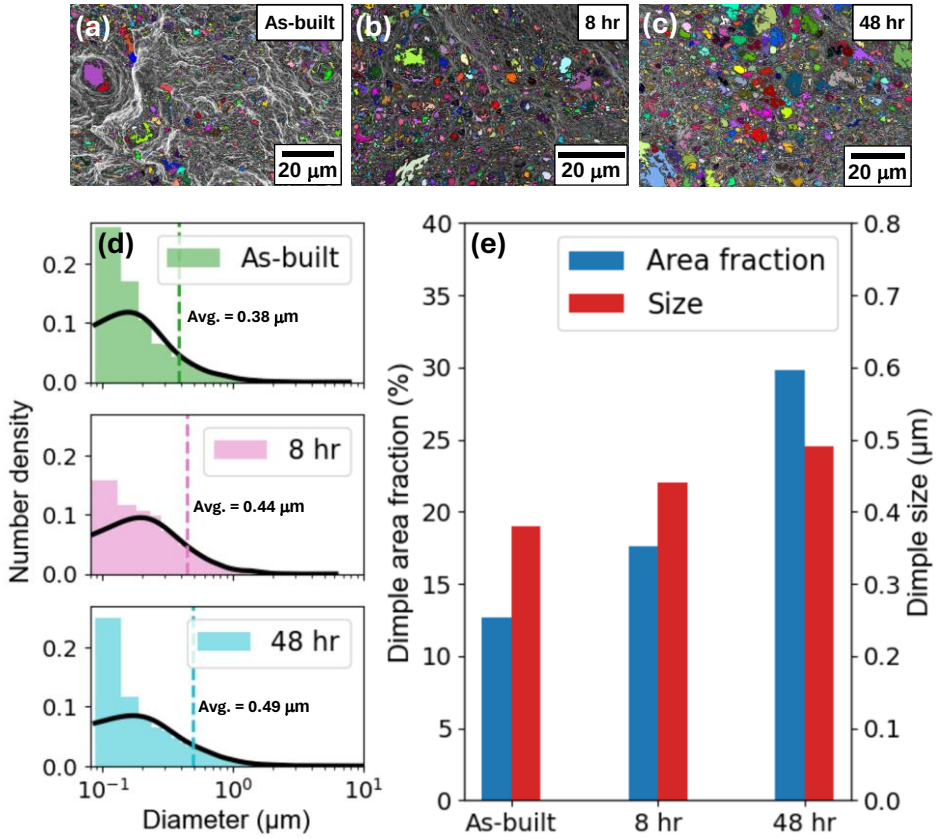

Fig. S1 (a–c) *Representative dimples identified using ImageJ in the as-built, 8-hour aged, and 48-hour aged samples, captured under the same field of view as in Fig. 2 of the main text.* ***(d)*** *Dimple size distribution across the three samples, showing that most dimples are smaller than 0.5 µm.* ***(e)*** *Evolution of dimple size and area fraction with aging time, demonstrating a clear increase in both metrics, consistent with the observed transition toward ductile fracture behavior.*

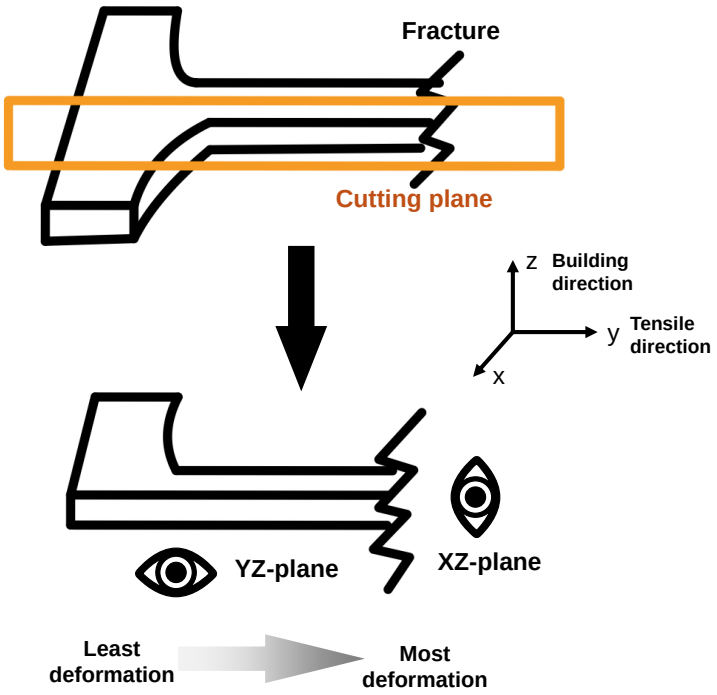

Fig. S2 *Schematic of sample preparation. Fractography analysis is conducted on the YZ and XZ plane. The YZ plane is exposed to evaluate microstructural deformation and cavity damage, with the degree of plastic deformation increasing progressively from the grip to the fracture point in the gauge.*

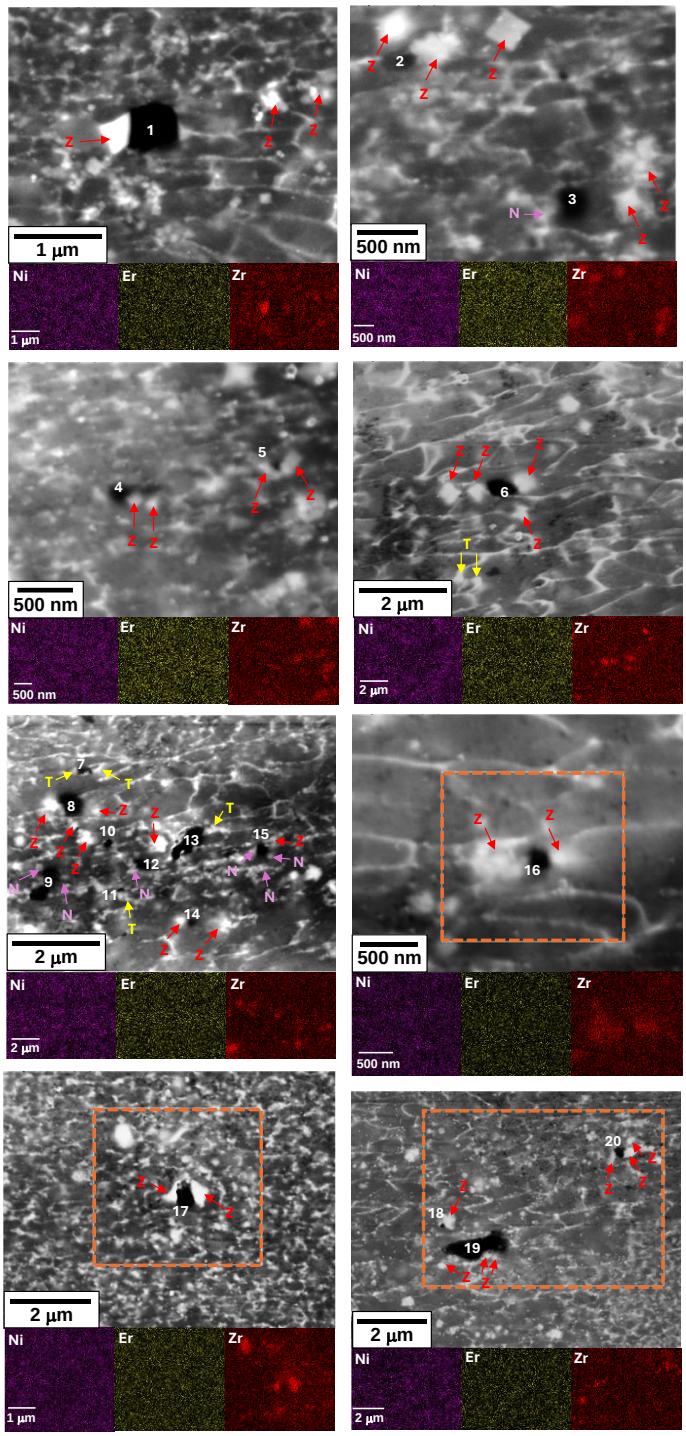

Fig. S3 *SEM-EDS on precipitates near cavity damages in* ***as-built*** *sample.*

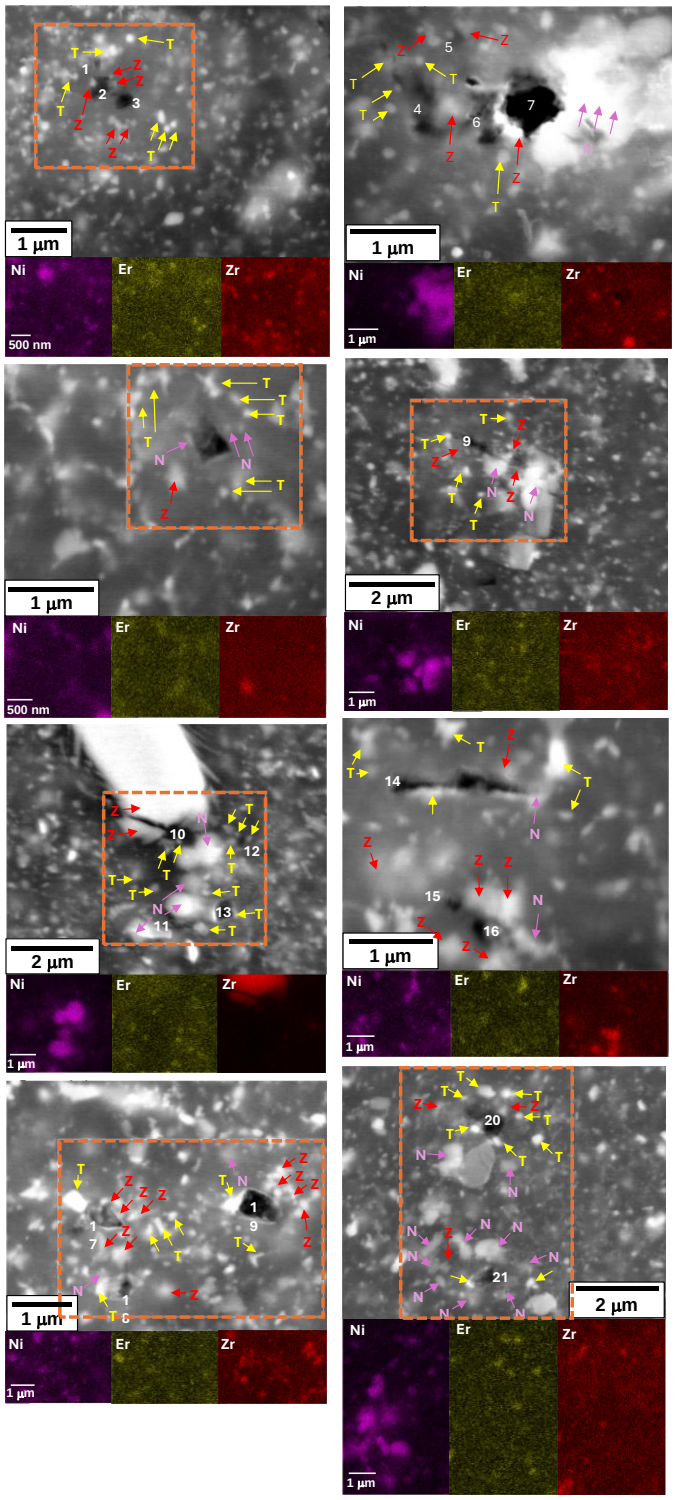

Fig. S4 *SEM-EDS on precipitates near cavity damages in* ***8-hour aging*** *sample.*

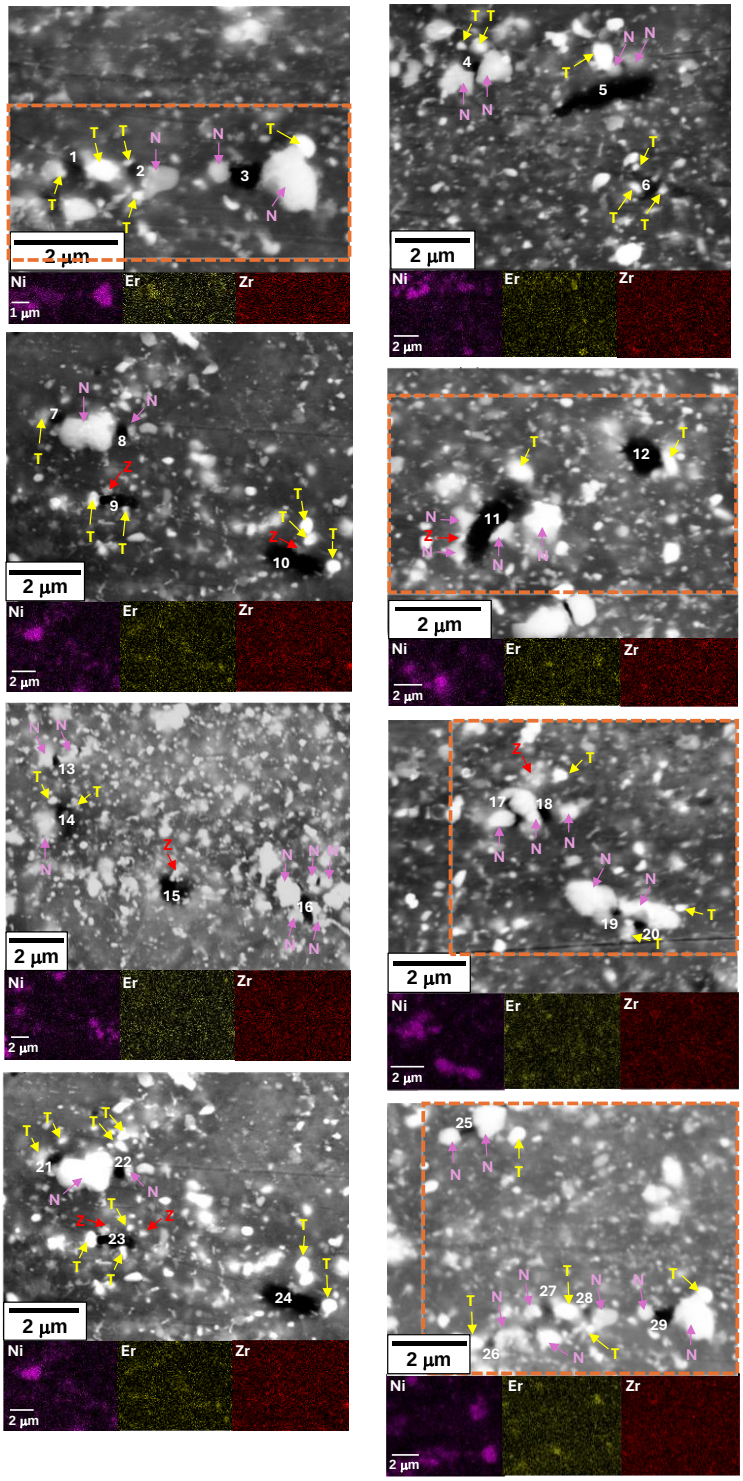

Fig. S5 *SEM-EDS on precipitates near cavity damages in* ***48-hour aging*** *sample.*

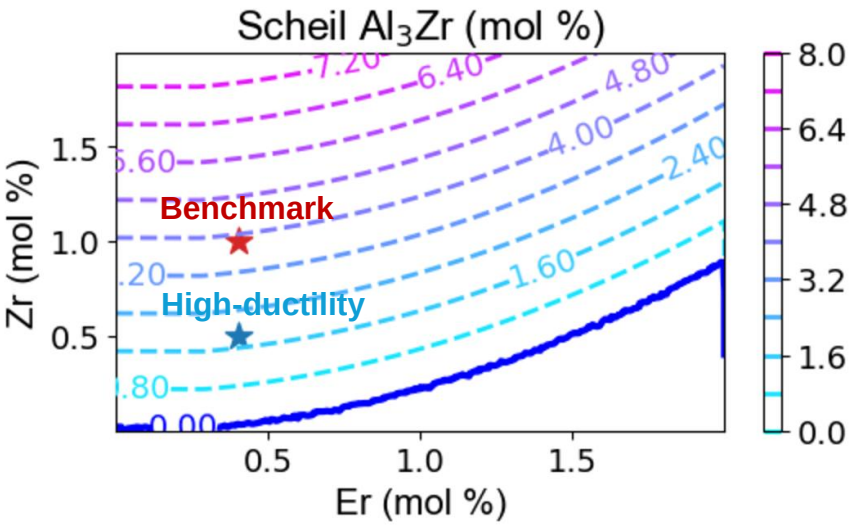

Fig. S6 *Contour plot of Al_3Zr in the Scheil simulation. As the Zr composition is reduced, the Al_3Zr-$D0_{23}$ phase decreases from 3.85 mol% to 1.83 mol%. The optimization was performed at single equilibrium condition, where Al_3Zr is nearly eliminated (Fig. 9). Future optimizations can be done to minimize Al_3Zr at Scheil conditions to better mimic as-built conditions and potentially further enhance ductility in the as-built state.*

Tables:

Table S1 *Mechanical properties of the samples at different aging time.*

	As-built	**8-hour aging**	**48-hour aging**
Yield strength (MPa)	391.23	406.55	355.03
Ductility (%)	0.93	3.97	6.43
Ultimate tensile strength (MPa)	395.87	410.28	358.44
Young's Modulus (GPa)	60.77	63.33	63.85

Table S2 *Dimple area fraction and equivalent diameter in the three samples.*

	As-built	**8-hour aging**	**48-hour aging**
Area fraction (%)	12.7	17.6	29.8
Size (μm)	0.38	0.44	0.49

Table S3 *Pettifor's Cauchy pressure and Pugh's ratio of binary Al precipitates*

	Pettifor's Cauchy pressure				**Pugh's ratio**			***Ref.***
	C_{11} **(GPa)**	C_{44} **(Gpa)**	E **(GPa)**	$\frac{C_{11}-C_{44}}{E}$	**G (Gpa)**	**B (GPa)**	$\frac{G}{B}$	
Al_3Zr ($D0_{23}$)	63	84	200.6	-0.105	85	103	0.825	[1], [2]
Al_3Ni	75	78	160.02	-0.0188	63	113	0.558	[1], [2]
Al_2Cu	58	61	131	-0.0229	50	111	0.450	[1], [2]
$Al_{11}Ce_3$	50	62	117	-0.106	47	75	0.630	[3]
Al_3Sc	44	69	159	-0.157	67	86	0.779	[1], [2]
Al_3Er	38	60	143	-0.154	60	77	0.779	[1], [2]
Al_3Mg_2	39	9	68	0.430	26	53	0.497	[4]
Al_6Mn	57	78	176	-0.119	71	111	0.640	[1], [2]
Al_6Fe	68	69	155	-0.00645	61	106	0.575	[1], [2]
Al_3Y	36	58	140	-0.157	59	75	0.787	[1], [2]
$AlTi_3$	82	59	155	0.148	61	114	0.535	[1], [2]
Al_2O_3	159	118	371	0.111	146	232	0.629	[1], [2]

Table S4 *Mechanical properties of benchmark and ductility-increased alloy at as-built condition*

	Benchmark	**Ductility-increased**
Yield strength (MPa)	391.23	283.48
Ductility (%)	0.93	15.49
Ultimate tensile strength (MPa)	395.87	295.09
Young's Modulus (GPa)	60.77	50.66

Reference:

[1] M. de Jong *et al.*, "Charting the complete elastic properties of inorganic crystalline compounds," *Sci Data*, vol. 2, no. 1, p. 150009, Mar. 2015, doi: 10.1038/sdata.2015.9.

[2] A. Jain *et al.*, "Commentary: The Materials Project: A materials genome approach to accelerating materials innovation," *APL Mater*, vol. 1, no. 1, Jul. 2013, doi: 10.1063/1.4812323.

[3] W.-J. Ding, J.-X. Yi, P. Chen, D.-L. Li, L.-M. Peng, and B.-Y. Tang, "Elastic properties and electronic structures of typical Al–Ce structures from first-principles calculations," *Solid State Sci*, vol. 14, no. 5, pp. 555–561, May 2012, doi: 10.1016/j.solidstatesciences.2012.02.006.

[4] B. Zheng, L. Zhao, X. B. Hu, S. J. Dong, and H. Li, "First-principles studies of Mg17Al12,Mg2Al3,Mg2Sn,MgZn2,Mg2Ni and Al3Ni phases," *Physica B Condens Matter*, vol. 560, pp. 255–260, May 2019, doi: 10.1016/j.physb.2018.11.067.